A Compressible Continuum Model for Ion Transport in High-Temperature Water

Caibin Xiao[†] and Robert H. Wood*

Department of Chemistry and Biochemistry, University of Delaware, Newark, Delaware 19716

Received: July 29, 1999; In Final Form: December 1, 1999

A compressible continuum model for the limiting electrical conductivity, Λ_0, is presented. Solvent density as a function of the radial distance r from a solvated, spherical ion is calculated via the compressible continuum model developed by Wood and co-workers. The viscosity of the solvent around an ion is calculated as a sum of electrostrictive and electroviscous components which are also taken as functions of r. The viscosity change due to electrostriction is obtained with the viscosity equation for water $\eta[\rho(r),T]$. Hubbard's expression for the electroviscous effect in an incompressible solvent is adapted to calculate the viscosity enhancement arising from the presence of an electric field at constant local solvent density. With only one adjustable parameter, this model reproduces, within experimental uncertainty, the experimental infinite dilution equivalent conductance data for aqueous NaCl from 140 to 800 °C at densities greater than 0.5 g cm^{-3}. Recent measurements of the Debye relaxation time allow this parameter to be eliminated with very small changes in the predictions. Below densities of 0.5 g cm^{-3}, the calculated values are too high by as much as 30%. For 140−800 °C and $1.0 > \rho_0 > 0.5$ g cm^{-3} the model correctly predicts that (1) Walden's rule is not obeyed, (2) Λ_0 varies linearly with density, (3) Λ_0 is a very weak function of temperature at constant density, and (4) for small ions ($r < 2$ Å) Λ_0 is a very weak function of ionic radius. Electrostriction and electroviscosity effects are shown to be very important in this region.

1. Introduction

The limiting electric conductance (Λ_0) of simple aqueous electrolytes is available over a wide range of temperature and pressure from extensive investigations by Noyes and co-workers,[1] Franck and co-workers,[2−7] Marshall and co-workers,[8−14] and by others.[15−20] The limiting conductance of ions can be used to calculate other ion transport properties through the Nernst−Einstein equation.[21] These experimental measurements reveal a very puzzling behavior for the high-temperature electrical conductance of aqueous ions. Marshall and co-workers in their series of publications exploring conductances of aqueous electrolytes found that Walden's rule ($\Lambda_0\eta_0 =$ constant, where η_0 is the bulk viscosity of the solvent) is not obeyed at high temperature. Instead of the expected behavior, they found that the limiting conductance was a linear function of the bulk density (ρ_0) of water for $0.5 < \rho_0 < 0.9$ g cm^{-3}. They used this linearity to extrapolate their data to conditions at which the limiting equivalent conductance was not accurately measured. Marshall and co-workers also found the limiting equivalent conductance Λ_0 was a very weak function of temperature. In contrast, Walden's rule suggests that the Walden product $\Lambda_0\eta_0$ and not Λ_0 itself should be a weak function of temperature.[22] Another curious feature of the experimental results is that the conductance of the alkali halides changes by less than 8% in the high-temperature region as the size of the ion changes by 70%, whereas in ambient conditions there are much larger differences.[19,20]

Although substantial progress has recently been made in the development of a quantitative molecular theory for limiting conductance,[23,24] these models require input parameters which can be difficult to extract from available experimental data. The semiempirical model of Oelkers and Helgeson[25] can be made to account for the above-mentioned puzzling behavior. Their model is based on the activation energy, E, for a jump of length l with an empirical temperature and pressure dependence and does not lead to any understanding of the reasons for the changes in E and l. The calculation of ion transport by a continuum electrohydrodynamic approach has a long history. Born first pointed out that dielectric relaxation in a polar solvent induced by a moving ion gives rise to the dielectric friction.[26] This friction is additional to the hydrodynamic friction considered in the Stokes' law model and helps explains the failure of Stokes' law for small ions. Born's model has been further extended and modified by Boyd,[27] Zwanzig,[28,29] and Hubbard and Onsager,[30,31] who considered various modes of coupling between hydrodynamic flow and the solvent polarization. Except for a first-order correction by Stiles and Hubbard,[32] these past continuum models for ionic mobility have neglected the compressibility of the solvent. In previous work from this laboratory it has been shown that the large change in density near the ion that arises from the high compressibility of the solvent can be accurately modeled using a compressible continuum (CC) model with dielectric saturation.[33,34] The goal of this work was to develop a compressible continuum model for calculating ionic mobility. It was our hope that electrostriction was the dominant additional effect at high temperatures so that a CC model would be reasonably accurate and explain the puzzling qualitative features Λ_0 as a function of temperature and density.

2. Compressible Continuum Model for Ionic Mobility

The compressible continuum model of Wood et al.[33,34] permits the calculation (in the continuum approximation) of the density,

* To whom correspondence should be addressed. E-mail rwood@udel.edu; FAX 302-831-6335.

[†] Current address: Chemical and Analytical Sciences Division, Oak Ridge National Laboratory, Oak Ridge, TN 37831.

10.1021/jp992675y CCC: $19.00
Published on Web 01/19/2000

ρ, dielectric constant, ϵ, and electric field, E, as functions of distance from the ion for a hard sphere ion in a compressible continuum solvent that has the properties of pure water. The details of this model have been given previously and will not be repeated here. Briefly, the model starts with the expression for the change in density with electric field at constant chemical potential of the solvent from Frank[35] and uses the expression of Quint and Wood[34] for the change in compressibility of the solvent with electric field at constant density. The dielectric saturation was estimated using Booth's equation[36] with the parameters adjusted to give the experimental value for the dielectric saturation of water at ambient conditions. Runge−Kutta numerical integration then yields the density and dielectric constant as a function of electric field. Using the law of Gauss, the distance from the ion, r, at which both this density and electric field, E, occur is given by $E = ze/(4\pi\epsilon_0\epsilon_r r)$. Wood et al.[33] compared this model with the results of simulation and experiment and found that it gave reasonable first coordination shells for the ions at high temperatures and that at very low densities ($\rho_0 \leq 0.01$ g cm^{-3}) the inclusion of dielectric saturation effects was important in order to obtain qualitative agreement with the simulations. This model did not give the enhanced density at large distances from the ion expected near the critical point presumably because fluctuations are neglected. More recently, Luo and Tucker have successfully applied this model (without dielectric saturation) to calculate the increased density of the solvent along the reaction path of a chloride ion with methyl chloride.[37,38]

To account for the inhomogeneous viscosity of the solvent in the vicinity of a ion, Wolynes suggested the following approximate relation for friction coefficient and limiting equivalent conductance Λ_0[39]

$$\Lambda_0 = \frac{Fe}{\xi} = Fe\int_R^\infty \mathrm{d}r/(4\pi r^2\eta(r)) = Fe\int_{1/R}^0 \frac{\mathrm{d}(1/r)}{4\pi\eta(r)} \quad (1)$$

where $\eta(r)$ is the radius-dependent viscosity, r is the distance from the center of the spherical ion, F is the Faraday, and R is the radius of the ion. Later, Brilliantov and Krapivsky[40] found that the eq 1 could be obtained from Navier−Stokes equation with the stick boundary condition if a homogeneous pressure field is assumed.

To calculate the limiting conductance from eq 1, we need to know the viscosity of the solvent near the ion as a function of the radial distance. We assumed that the total viscosity can be expressed as a sum of an electrostriction (ES) and an electroviscous (EV) effect.

$$\eta[\rho(r),T,E(r)] = \eta_{ES}[\rho(r),T,0] + \Delta\eta_{EV}[\rho(r),T,E(r)] \quad (2)$$

The first term η_{ES} is the viscosity of water at $\rho(r)$ and T in the absence of an electric field. This is calculated from an equation of state for the viscosity of pure water[41] as a function of density and temperature,

$$\eta_{ES}(r) = \eta[\rho(r),T] \quad (3)$$

with $\rho(r)$ calculated from the CC model.[33] The second term $\Delta\eta_{EV}$ is the change in viscosity when an electric field is applied at constant T and ρ.

For a steadily moving ion, Hubbard and Onsager[30] have shown that the dielectric relaxation induced by the motion of the ion leads to an electroviscous effect, i.e., an enhancement of fluid viscosity by the electric field. In the case of a constant velocity gradient flow in a uniform electric field, Hubbard[31,39] gave $\Delta\eta_{EV}(r)$ as

$$\Delta\eta_{EV}(r) = \tau_D\epsilon_0(\epsilon_r(r) - \epsilon_\infty)E(r)^2/4 \quad (4)$$

where τ_D is the Debye relaxation time of the solvent, ϵ_r and ϵ_∞ are the static and the optical dielectric constants, respectively, and ϵ_0 is the permittivity of free space. We assume this equation is valid for a compressible solvent at constant density. We estimate τ_D from the viscosity of water by the following Debye−Einstein−Stokes equation:

$$\tau_D(r) = 4\pi\eta_{ES}(r)R_w^3/k_BT \quad (5)$$

where R_w is the hydrodynamic radius of a rotating molecule and k_B Boltzmann's constant. Rønne et al.[42] have shown that this equation holds for water at temperatures up to 366 K. We adapt eqs 5 and 6 for the compressible solvent by assuming all the variables in these equations could take their local values. Combining eqs 2, 4, and 5, we have

$$\eta(r) = \eta_{ES}[\rho(r),T](1 + \pi R_w^3\epsilon_0[\epsilon_r(r) - \epsilon_\infty]E(r)^2/k_BT) \quad (6)$$

Given $\eta(r)$, the limiting ionic conductance is simply obtained from eq 1.

Computation. To calculate the limiting conductance for NaCl from the friction with the present model, we first calculate $\rho(r)$, $\epsilon_r(r)$, ϵ_∞, and $E(r)$ from the CC model of Wood et al.[33] For a given $\rho(r)$, $\eta_{ES}(r)$ is calculated from the equation of state for the viscosity of water given by Kestin et al.[41] For a small region very close to the surface of the ion the densities are beyond the domain of validity of this equation. Under these conditions, $\eta_{ES}(r)$ was extrapolated using the linear relation:

$$1/\eta_{ES} = a + b/\rho \quad (7)$$

where a and b are two constants determined with viscosity values from Kestin et al.'s equation at $p = 400$ and 500 MPa for $T \leq 674$ K and at $p = 300$ and 350 MPa at $T > 674$ K. It was confirmed by Loef[43] that eq 8 could be used to interpolate the viscosity data for water at elevated temperatures. This extrapolation has little effect on our results since eq 8 is only needed for viscosities in a small region very close to the surface of the ion. Any reasonable extrapolation would give conductances within 2% of the results reported here.

Before we substitute eq 7 into eq 1 and carry out the integration numerically, we have to know R for the ions and R_w for water. We use the crystallographic radius for sodium ion and chloride ion, i.e., $R(Na^+) = 0.98$ Å and $R(Cl^-) = 1.86$ Å, and treat R_w as the only adjustable parameter in our calculation. R_w is adjusted to 1.66 Å using the experimental Λ_0 at $T = 634.89$ K and $\rho_0 = 0.5503$ g cm^{-3}.[20] This value of R_w is quite reasonable but higher than $R_w = 1.372$ Å obtained from τ_D of water in the temperature range $271 < T < 367$ K by Rønne et al.[42] from the experimental real and imaginary part of the dielectric constants.

3. Discussion

A. Prediction of Λ_0 for NaCl. The calculated Λ_0 for $NaCl_{(aq)}$ are shown in Figure 1 along with the experimental data from this laboratory[19,20] (579 K $< T <$ 678 K, 0.2 g cm^{-3} $< \rho_0 <$ 0.7 g cm^{-3}), Noyes and co-worker (T = 413.15, 429.15, 491.15, 554.15, and 579.15 K at saturation pressures),[1] and the compilation of Quist and Marshall (T = 473.15 and 573.15 K at saturation pressures).[44] Figure l shows experimental equivalent

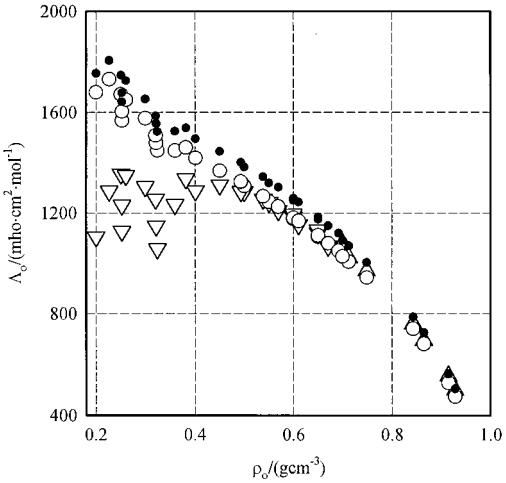

Figure 1. Limiting equivalent conductance, Λ_0(NaCl, aq), as a function of density of the solvent at various temperatures from 413 to 673 K and low pressures (the saturation pressure to 28 MPa): ▽, Zimmerman et al.[19] and Gruszkiewicz and Wood;[20] △, Noyes[1] at T = 413, 429, 491, 554, and 579 K and the saturation pressures and Quist and Marshall[44] at T = 473 and 573 K and the saturation pressures; ○, this model with R_w = 1.66 Å at the corresponding experimental conditions; ●, this model with R_w = 1.4 Å (ρ_0/1 g cm^{-3})$^{-1.24/3}$. At density greater than 0.5 g cm^{-3}, the temperature dependence of Λ_0 at a constant density is very small but substantial at lower densities as evidenced by the scatter at low densities.

conductances at temperatures form 413 to 677 K. Predictions are essentially within experimental accuracy at all densities above 0.5 g cm^{-3}. The model also predicts that in this region the limiting conductances are not strong functions of either the pressure or the temperature, just the density. At water densities less than 0.5 g cm^{-3} the model predictions are too high by increasing amounts with errors as large as 50% at ρ_0 = 0.2 g cm^{-3}. The model correctly predicts a pronounced temperature dependence of Λ_0 at low densities. A similar but larger temperature dependence occurs in the experimental data, and this is what produces the scatter in Figure 1 at $\rho_0 \leq$ 0.4 g cm^{-3}. In Figure 2 the calculated Λ_0 for NaCl is compared with experimental results from Ho and Palmer[18] and Quist and Marshall[12] at very high temperatures. The model correctly predicts the very weak temperature dependence of Λ_0 at constant density in this region. In fact, with one adjustable parameter, R_w, the present CC model can fit all of the experimental conductance data at densities greater than 0.4−0.5 g cm^{-3} with an accuracy about equal to the experimental error.

After these calculations were completed some new measurements of τ_D in the supercritical region were reported by Okada et al.[45,46] Their measurement of τ_D can be reproduced by R_w = 1.4 Å (ρ_0/1 g cm^{-3})$^{-1.24/3}$. Figure 1 shows that this value of R_w gives a prediction of conductance which is slightly higher than when R_w = 1.66 Å, but there are no adjustable parameters in this prediction of Λ_0. Both models for R_w have no temperature dependence so the agreement will be similar at other temperatures. The predicted conductances are very similar even though the experimental τ_D is much higher below 0.5 g cm^{-3} because the electroviscous effect is important only when the electric field (and therefore density) is high (r < 5 Å). The average τ_D at densities from 0.5 to 0.8 g cm^{-3} are very similar for the two models of R_w and thus give similar predictions of Λ_0. For the present purpose of exploring the reasons for the unusual behavior of Λ_0 at high temperature, either model is good enough so we will only discuss the R_w = 1.66 Å model.

Figure 3 shows experimental and calculated Walden products, $\Lambda_0\eta_0$, at temperatures near 652.0 and 1073.15 K as a function

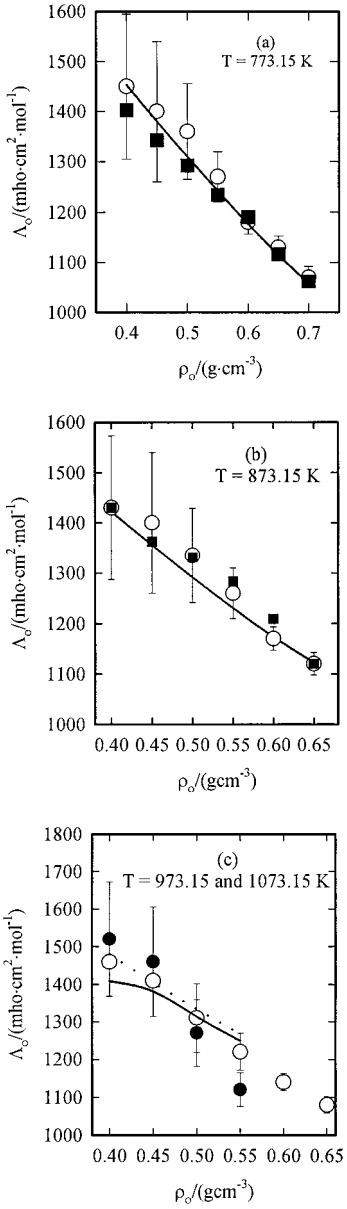

Figure 2. Comparison of Λ_0(NaCl, aq) predicted by this model with the experimental results of Quist and Marshall[12] at $T \geq$ 773 K: For plots a and b: lines, this model; ○, Quist and Marshall[12] with their estimated error bars; ■, Ho and Palmer[18] (their estimated errors are about the same as Quist and Marshall's). For plot c: dashed line, this model for T = 1073.15 K; solid line, this model for T = 973.15 K; ○, Quist and Marshall[12] at T = 973.15 K; ●, Quist and Marshall[12] at T = 1073.15 K. The model correctly predicts that the temperature dependence at these densities is very small.

of density. The present model predicts a decrease in $\Lambda_0\eta_0$ with decreasing density and then an upturn below ρ_0 = 0.2 g cm^{-3}. Unfortunately, there are no experimental data with which to test the prediction of an upturn, but we can explore the reasons for this prediction. The drop in $\Lambda_0\eta_0$ indicates an increase in the size of the hydration sphere as the density drops. Gruszkiewicz and Wood[20] pointed out that the temperature and density dependence of this effect indicated it was not a critical scaling effect and suggested the longer ranged hydration was due to (1) the lower dielectric constant at low densities which increases the electrostatic forces on the water and (2) the increase in $\rho(r)/\rho_0$ at a larger distance from the ion as the bulk density decreases, indicating that more water should be carried along. Recent molecular dynamics simulations of Lee et al.[47] are in accord with this explanation. Lee et al.[47] found that ion−water

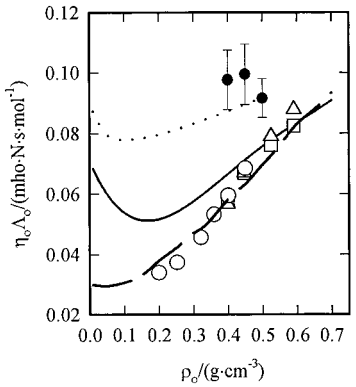

Figure 3. Values of $\Lambda_0\eta_0$(NaCl, aq) as a function of density of the solvent at T near 652 K and at 1073.15 K: solid line, this model at T = 652.5 K; dotted line, this model at T = 1073.15 K; ○, T near 652 K from Gruszkiewick and Wood;[20] △, Pearson et al.,[17] T = 656.15 K; □, Pearson et al., T = 651.15 K; ●, Quist and Marshall[12] at T = 1073.15 K; long dashed line, prediction of Oelkers and Helgeson from fitting the experimental results with a semiempirical equation.[25] The viscosities of water at these conditions were calculated from an equation by Kestin et al.[41]

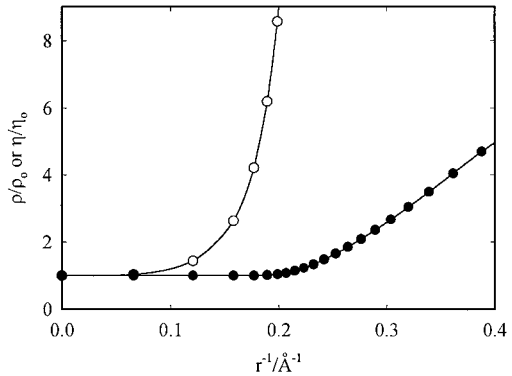

Figure 4. Comparison of $\rho(r)/\rho_0$ with $\eta(r)/\eta_0$. At T = 656.0 K and ρ_0 = 0.01 g cm^{-1}, the local density of water near the ion is greatly enhanced (show as open circles) while the enhancement of the local viscosity is much less (shown as dots).

potential energies increased with decreasing density, and the equivalent conductances of their model are in agreement with experiment.[19,20] Unfortunately, the simulations were limited to $\rho_0 > 0.2$ g cm^{-3}. Why then is there an upturn in $\Lambda_0\eta_0$ below ρ_0 = 0.2 g cm^{-3} when simulations[33] and the present model show an increasing size of the hydration sphere even at ρ_0 = 0.01 g cm^{-3}? The answer is that the viscosity of the solvent is no longer roughly proportional to the bulk density of the solvent below ρ_0 = 0.2 g cm^{-3}. Figure 4 shows that for R between 10 and 5 Å η_{ES} is essentially constant, while the density increases dramatically. Thus, that part of the hydration sphere with density less than 0.2 g cm^{-3} does not affect the conductance, and the present compressible continuum model predicts an upturn. Kinetic theory[48] shows that ion mobility in a gas is inversely proportional to the density of the gas so that Λ_0 goes to infinity as density goes to zero. (At ρ = 0, there are no collisions so the ion never stops accelerating in the electric field.)

The predictions of the semicontinuum model of Balbuena et al.[49] using rotational correlation times from a computer simulation are too high at 28 MPa by about 30% at ρ_0 = 0.7 g cm^{-3} and by about 70% at ρ_0 = 0.28 g cm^{-3}. The semiempirical model of Oelkers and Helgeson predicts the density dependence quite well but as pointed out above does not explain what causes the density dependence.[25]

B. Comparison with the Hubbard−Onsager and Zwanzig Model. To compare with the Hubbard−Onsager theory,[30,31] we

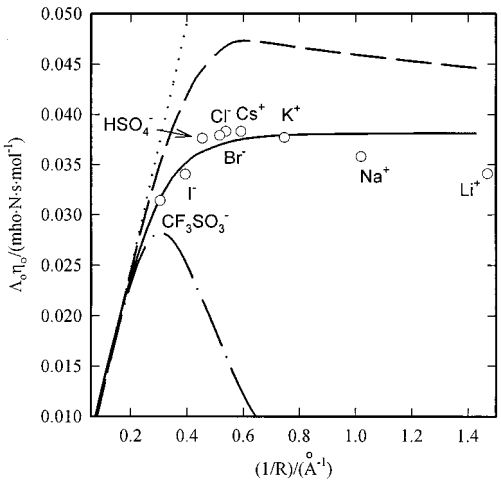

Figure 5. Values of $\Lambda_0\eta_0$ of univalent ions in water at T = 655.91 K and p = 28.0 MPa (ρ_0 = 0.4930 g cm^{-3}) plotted as a function of the inverse of the crystallographic ionic radius 1/R: The dotted line represents the predictions of Stokes' law, the large-dashed line Hubbard−Onsager theory, and the dot dashed line Zwanzig theory. The solid line shows the results from the present model. The open circles are for ions; the value of λ_0 for an individual ion is obtained based on the assumption of $\lambda_0(Cs^+) = \lambda_0(Br^-)$ since their radii are close. λ_0 for $CF_3SO_3^-$ and K^+ were calculated from Λ_0 for $NaCF_3SO_3$ and KCl at T = 655.91 K and p = 28.0 MPa which are interpolated from the tables reported by Ho and Palmer.[51,52] λ_0 for HSO_4^- and I^- were calculated from Λ_0 of $KHSO_4$ and NaI at T = 655.91 K and p = 28 MPa which are interpolated from the tables by Quist et al.[10] and Dunn et al.[8] Values for the crystallographic radius R are taken from the compilation of Shock and Helgeson.[53] The radius for $CF_3SO_3^-$ is estimated from the density of liquid triflic acid at 25.0 °C.[54] R_w = 1.66 Å was used for all three models.

obtained the friction coefficient using the numeric solution of the Hubbard−Onsager equations which has been fitted into a polynomial by Ibuki and Nakahara.[50] It was found that the Hubbard−Onsager theory and the Zwanzig model[28,29] can be fitted into the experimental data for NaCl at a single temperature by adjusting R_w. However, unlike the present model, a single R_w cannot reproduce the experimental data at other temperatures without changing R_w. If R_w is adjusted to fit the data at 473.15 K and ρ_0 = 0.864 g cm^{-3}, the predictions of the Hubbard−Onsager theory are off by as much as 16% and those of Zwanzig by 22% at the highest temperatures (1073 K and ρ_0 = 0.50 g cm^{-3}). With our estimate of R_w, the Hubbard and Onsager predictions for NaCl are too high at this temperature and Zwanzig model is too low, whereas the present model predictions are quite accurate.

The Walden product as a function of the ionic size at 655.91 K and 28 MPa is presented in Figure 5. All three models give the correct (Stokes−Einstein) ionic size dependence for relatively large ions, and the current model inherits the electrohydrodynamic saturation effect for small ions from the Hubbard−Onsager theory.[30,31] The Zwanzig model has a wrong 1/r dependence due to an electroviscous effect that is too large. If a much larger R_w = 2.2 Å is used, the Hubbard−Onsager theory reproduces the 1/r dependence for small ions (K^+, Na^+, and Li^+) very well.

C. Discussion of the Continuum Model. The continuum model is surprisingly accurate over a very wide temperature and density range considering the approximations that have been made in deriving it. At low temperatures (below 100 °C) the model fails, but this is not surprising given the anomalous structure effects present in low-temperature aqueous solutions (for instance, the decrease in viscosity as the larger alkali halides

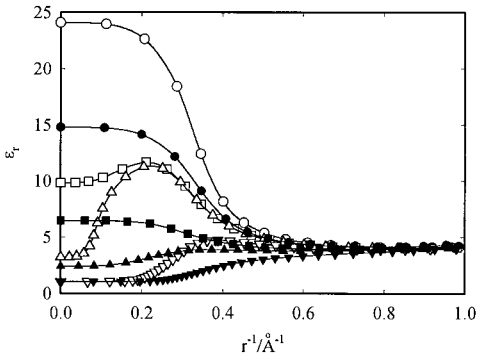

Figure 6. Plot of dielectric constant as a function of $1/r$ at $T = 656.0$ K (open symbols) and $T = 973.0$ K (filled symbols): ○ and ●, $\rho_0 = 0.9$ g cm^{-3}; □ and ■, $\rho_0 = 0.493$ g cm^{-3}; △ and ▲, $\rho_0 = 0.2$ g cm^{-3}; ▽ and ▼, $\rho_0 = 0.01$ g cm^{-3}.

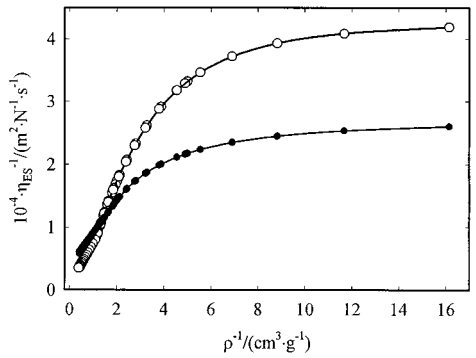

Figure 7. Plot of the reciprocal of the electrostriction viscosity, η_{ES}-(r), vs the reciprocal of the density of water at that radius at $T = 656.0$ K (open symbols) and $T = 973.0$ K (filled symbols).

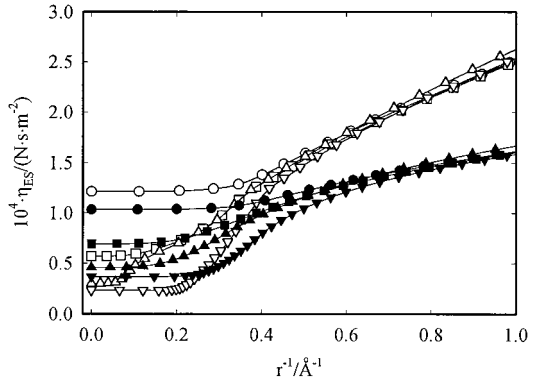

Figure 8. Plot of the electrostriction viscosity, $\eta_{ES}(r)$, as a function of $1/r$ at $T = 656.0$ K (open symbols) and $T = 973.0$ K (filled symbols): ○ and ●, $\rho_0 = 0.9$ g cm^{-3}; □ and ■, $\rho_0 = 0.493$ g cm^{-3}; △ and ▲, $\rho_0 = 0.2$ g cm^{-3}; ▽ and ▼, $\rho_0 = 0.01$ g cm^{-3}.

are added to water). At higher temperatures we can look at the continuum model predictions of ϵ, η_{ES}, η_{EV}, and Λ_0 to gain insight into the effects responsible for the successful prediction of the trends in conductance at densities above 0.4−0.5 g cm^{-3} and the failure of the model at lower densities. In particular, we want to know the reason for the failure of Walden's rule at high temperatures and for the almost constant values of Λ_0 as functions of the radius of the ion for alkali halides. We find that there is no single effect that explains all of these trends but that electrostriction, electroviscosity, and dielectric saturation all have important effects.

To explore the trends versus temperature and density, we have used the model to predict the properties of water as a function of the distance from the ion at temperatures of 656 and 973 K and bulk water densities from 0.9 to 0.01 g·cm^{-3}. It is instructive to start by examining the continuum predictions of the dielectric constant, ϵ_r. Figure 6 shows a plot of $\epsilon_r(r)$ as a function $1/r$. One of the most striking features of this plot is that, inside about 1.5 Å, ϵ_r is independent of the temperature and bulk density of the solvent. Presumably this is due to dielectric saturation, and the value of ϵ_r (≈4.2) is the contribution of the polarizability of the water to the dielectric constant. At 973 K the dielectric constant starts at its bulk value far from the ion and monotonically either decreases or increases to the saturation value at low radii with the transition occurring between about 2−5 Å. At low temperatures and the two intermediate densities ($\rho_0 = 0.493$ and 0.200 g cm^{-3}) the dielectric constant rises above its bulk value due to the electrostriction and then drops to the polarizability value at small radii where dielectric saturation dominates. At 656 K the electrostriction effect is most pronounced at $\rho_0 = 0.2$ g cm^{-3}, and the effect occurs at long distances from the ion (from above 10 Å to perhaps 3 Å), indicating that at this temperature and density there is long-range hydration around the ion. This is not surprising since at 656 K and $\rho_0 = 0.2$ g·cm^{-3} the solvent is compressible, and nearer to the ion the density increases and the bulk solvent becomes even more compressible before becoming less compressible as the density increases above 0.32 g cm^{-3}. It seems likely that the temperature dependence of the compressibility (and therefore the long-range hydration) is responsible for the stronger dependence of both calculated and experimental Λ_0 on temperature in this region (see Figure 1).

Figure 7 shows the reciprocal of the electrostriction viscosity, η_{ES}, vs the reciprocal of the density of the solvent at that radius. As expected, all of the points for the low temperature follow one line and all the points for the highest temperature follow another line since this is just the viscosity of pure water versus ρ_0 at two temperatures. On this plot our extrapolation of the viscosity equation is shown by the extrapolation to densities greater than about 0.95 g cm^{-3} at 656 K and 0.66 g cm^{-3} at 973 K. Reasonable differences in the extrapolation to higher densities make only rather small contributions to the predicted equivalent conductances (<1.0% at $T \approx 673$ K). At lower densities ($\rho_0 = 0.1-0.01$ g cm^3) η_{ES} becomes almost independent of density. At low temperatures the viscosity is about 2.5×10^{-5} Pa·s in this region, and at high temperature it is 3.9×10^{-5} Pa·s.

Figure 8 shows a plot of η_{ES} as a function of $1/r$. Inside about 2 Å the electrostrictive viscosity is independent of the bulk density but different at the two temperatures. The long-range hydration at $T = 656$ K and $\rho_0 = 0.2$ g cm^{-3} is evident in the bump in η_{ES} starting at about 10 Å. Figure 9 shows the total viscosity ($\eta = \eta_{ES} + \Delta\eta_{EV}$) as a function of $1/r$. The same long-range hydration is present, and inside 2 Å the total viscosity is also independent of the bulk viscosity at both temperatures. Comparison of Figures 8 and 9 shows that for radii larger than 5 Å electrostriction accounts for almost the total viscosity whereas near 2.5 Å the two make about equal contributions to the total viscosity, and below 1.5 Å electroviscosity is the dominant effect ($\Delta\eta_{EV} \gg \eta_{ES}$). The importance of $\Delta\eta_{EV}$ was investigated by a calculation of Λ_0 of NaCl in Figure 1 with $\Delta\eta_{EV} = 0$. The resulting Λ_0's are too high by about 30% at all densities, showing the importance of the electroviscous effect.

Next we explore the contribution of $\eta(r)$ to the total limiting equivalence conductance. To do this, we plot the integrand in the right-hand side of eq 1 ($I = Fe/4\pi\eta(r)$) as a function of $1/r$. The area under this curve from 0 to $1/R$ gives the equivalent conductance of a hard sphere ion of radius R. The plot of I vs $1/r$ is shown in Figure 10. If there were no electrostriction or

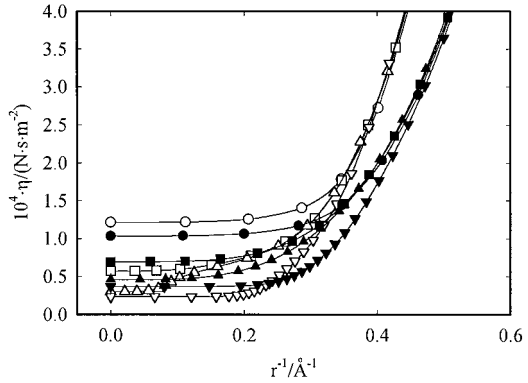

Figure 9. Plot of the total, $\eta_{ES}(r) + \eta_{EV}(r)$, as a function of $1/r$ at $T = 656.0$ K (open symbols) and $T = 973.0$ K (filled symbols): ○ and ●, $\rho_0 = 0.9$ g cm^{-3}; □ and ■, $\rho_0 = 0.493$ g cm^{-3}; △ and ▲, $\rho_0 = 0.2$ g cm^{-3}; ▽ and ▼, $\rho_0 = 0.01$ g cm^{-3}.

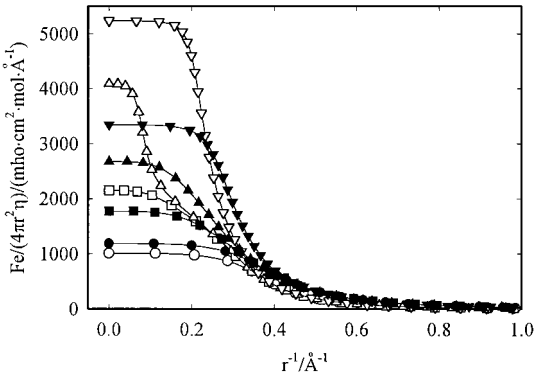

Figure 10. Plot of the integrand in the right-hand side of eq 1 as a function of $1/r$ at $T = 656.0$ K (open symbols) and $T = 973.0$ K (filled symbols): ○ and ●, $\rho_0 = 0.9$ g cm^{-3}; □ and ■, $\rho_0 = 0.493$ g cm^{-3}; △ and ▲, $\rho_0 = 0.2$ g cm^{-3}; ▽ and ▼, $\rho_0 = 0.01$ g cm^{-3}.

electroviscosity effects, the continuum model would predict that this integrand was a constant outside the radius of the ion and so the equivalent conductance is the integrand times $1/R$, and this is just Stokes' law with the stick boundary condition for an incompressible continuum solvent with no electroviscosity. Figure 10 shows that this primitive continuum model fails between 15 and 5 Å depending on the temperature and density. The contribution of the region inside 2.5 Å to the conductance of the ion is (1) rather small because the viscosity close to the ion is so high that it contributes little to the conductance (that is why the alkali halides have conductances that are substantially independent of radii in this region), (2) independent of the bulk density because of the high electrostriction, and (3) only slightly dependent on the temperature. If we multiply all of the curves in Figure 10 by the bulk viscosity, then the $1/r = 0$ intercepts are all equal, and the integral under the curve is the Walden product ($\Lambda_0\eta_0$). Failure of Walden's rule occurs when the cures drop below their $1/r = 0$ intercepts. This plot predicts clearly that Walden's rule is obeyed outside 10 Å (except at 656 K and $\rho_0 = 0.2$ g cm^{-3} where it fails at about 20 Å) and indicates that the failure of Walden's rule is mainly due to electrostriction and electroviscosity effects.

Figure 11 shows the calculated Walden product ($\Lambda_0\eta_0$) as a function of $1/r$. The linear region at large radius is the Stokes' law region, and the bend over to a relatively flat curve yields the independence of both Walden product and equivalent conductance with radius for small ions. The long-range hydration at 656 K and $\rho_0 = 0.2$ g cm^{-3} is evident in the early deviation from the Stokes' law. Except at 656 K and $\rho_0 = 0.2$ g cm^{-3}, ions with radii greater than about 10 Å obey the Walden product

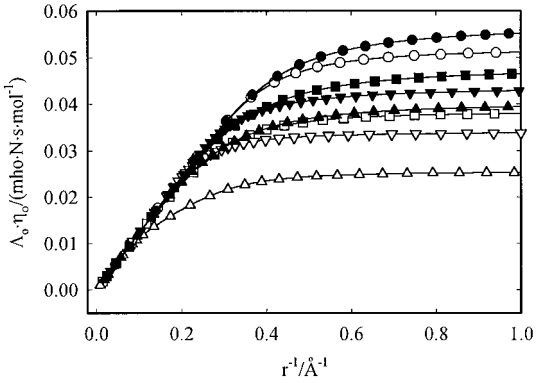

Figure 11. Plot of the calculated Walden product as a function of $1/R$, where R is the radius of the ion at $T = 656.0$ K (open symbols) and $T = 973.0$ K (filled symbols): ○ and ●, $\rho_0 = 0.9$ g cm^{-3}; □ and ■, $\rho_0 = 0.493$ g cm^{-3}; △ and ▲, $\rho_0 = 0.2$ g cm^{-3}; ▽ and ▼, $\rho_0 = 0.01$ g cm^{-3}.

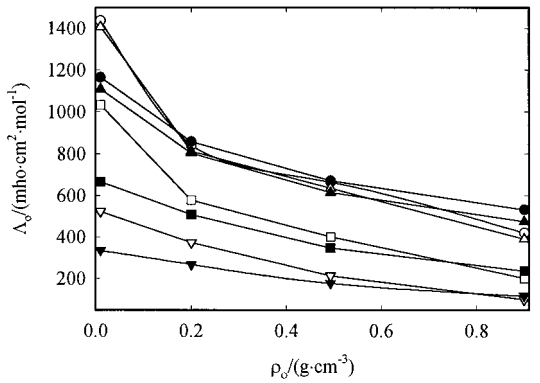

Figure 12. Plot of the equivalent conductance as a function of the bulk density of water for 1, 2, 5, and 10 Å ions at $T = 656.0$ K (open symbols) and $T = 973.0$ K (filled symbols): ○ and ●, $R = 1.0$ Å; △ and ▲, $R = 2.0$ Å; □ and ■, $R = 5.0$ Å; ▽ and ▼, $R = 10.0$ Å.

very accurately at any temperature and density. This is a clear prediction of the present model. Unfortunately, there are no data on very large ions at high temperatures with which to test this prediction. Figure 12 gives a plot of the equivalent conductance as a function of the bulk density of water for 1, 2, 5, and 10 Å ions. For the small ions (1 and 2 Å) the equivalent conductance is not a strong function of temperature or ion radius, and it is not far from linear in density down to $\rho_0 = 0.2$ g cm^{-3}. At lower densities the equivalent conductance goes up. The linearity in density was observed by Quist and Marshall down to about $\rho_0 = 0.5$ g cm^3.[11−14] More recent experimental measurements[19,20] as well as the molecular dynamics simulations of Lee et al.[47] indicate that the slope of equivalent conductance versus density below $\rho_0 = 0.5$ g cm^{-3} changes, and the present model fails in this region. Figure 13 gives a plot of the Walden product $\Lambda_0\eta_0$ versus density for the same ion sizes. For the 10 Å ions the Walden product is independent of temperature and independent of bulk density except that at $\rho_0 = 0.9$ g cm^{-3} the Walden product is a little higher. At 5 Å the Walden product is independent of temperature and bulk density except for the point at 656 K and $\rho_0 = 0.2$ g cm^{-3}. The deviation of this point is undoubtedly due to the long-range hydration shown above under these conditions. For the smaller ions (1 and 2 Å), the Walden product is a function of temperature but not a strong function of the ion size, and it is not far from linear in the 0.9−0.2 g cm^{-3} region and increases at lower densities.

Lee et al.[47] attribute the nonlinearity in Λ_0 as a function of density from 0.8 to 0.2 g cm^{-3} at 400 °C to changes in the number of water molecules in the first hydration sphere of the

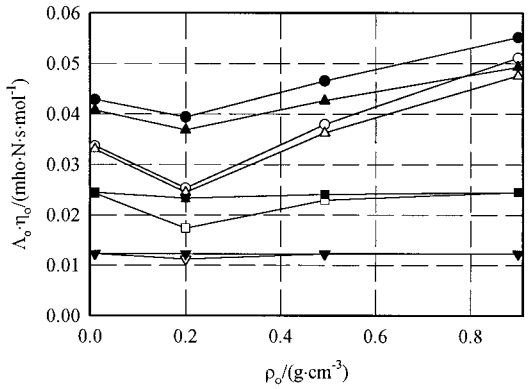

Figure 13. Plot of the calculated Walden product $\Lambda_0\eta_0$ as a function of the bulk density of water for 1, 2, 5, and 10 Å ions at $T = 656.0$ K (open symbols) and $T = 973.0$ K (filled symbols): ○ and ●, $R = 1.0$ Å; △ and ▲, $R = 2.0$ Å; □ and ■, $R = 5.0$ Å; ▽ and ▼, $R = 10.0$ Å.

ions and the interaction between the ions and these waters. While the effects discussed by Lee et al. are undoubtedly important in determining Λ_0 (and these effects may not be accurately modeled by the compressible continuum approximation), the present approach shows that the change in the bulk viscosity alone with no change in the effective Stokes radius of an ion would cause a nonlinear increase in Λ_0 at 0.8 g cm^{-3} by a factor of 2 at 0.5 g cm^{-3} and a factor of 5 at 0.2 g cm^{-3}. Thus, a very large increase in the local viscosity (Stokes radius) is needed to counterbalance this large decrease in viscosity. The present compressible continuum model does not have a large enough increase in local viscosity in the density range 0.5−0.2 g cm^{-3} to give good predictions. However the present model indicates that a majority of the difference between the conductance at 0.5 and 0.2 g cm^{-3} at this temperature is due to changes in local viscosity outside 4 Å, indicating that long-range effects cannot be ignored in any quantitative model. Simulations at densities of 0.22 and 0.01 g cm^{-3} show long-range hydration in qualitative support of this conclusion.[20,47]

The present continuum theory neglects the direct effect of the increased attraction between smaller ions and the first solvation shell on the mobility but does include the density changes and resulting viscosity increases in the solvent due to the increased electric field in the first solvation shell. Thus, it includes only one of the effects in the "solventberg" model[45,46] and a continuum approximation to dielectric friction. For a relatively incompressible solvent one should expect failure of the present model, and indeed it does fail in water below about 140 °C. The success of the present model in a compressible solvent indicates the neglected effect is small in this solvent.

Because of the crudeness of the present model, there are many possible reasons for its failure to predict Λ_0 of alkali halides at densities less than 0.4−0.5 g cm^{-3}. Some of the most likely possibilities are discussed below:

First, since this is a continuum model, the molecular nature of the ion motion in a polar solvent is totally neglected. Recent molecular theories of the dielectric friction[23,24,39,55−57] and computer simulations of molecular dynamics of the motion of an ion[23,24,47,49,58−63] show that the structure of the solvent around the ion and the nature of motion of solvent molecules particularly in the first solvation shell need to be considered in explaining the puzzles of the mobility of small ions in polar solvents. The number of molecules in the first solvation sphere is dropping so molecular effects could easily be important. One possible way of accounting for the molecular nature of the solvent in the first solvation shell would be to use the semicontinuum model of Balbuena et al.[49] for the first shell and the present model for the outer shells where the compressible continuum model should be more accurate. Combining the two models in such a way yields Λ_0 closer to the experimental values, but the contributions are too small so that the predictions are still much higher than both the experimental results and the simulations of Lee et al.[47]

Other possible reasons for the failure of the present model are discussed below. The electroviscosity calculation at low densities may be wrong. The electric fields are much higher at low densities due to the lower dielectric constant so errors may be higher. We have estimated the dielectric saturation from experimental measurements at room temperature, and the use of this estimation at extremes of temperature and very low densities may be in error. A single calculation for the Cl^- ion at 673 K showed that, with no dielectric saturation, the predicted equivalent conductance increased by 10−15% at most densities except for a dip in the 0.25−0.35 g cm^{-3} region where the increase was 0−5%. A lower dielectric saturation may improve the predictions of this model but would involve introducing another adjustable parameter, and this was beyond the scope of the present investigation.

A complete electrohydrodynamic equation should be used to investigate the influence of the electrostriction on ionic mobility. In addition to the dielectric relaxation, the motion of an ion in a compressible solvent also induces a translational relaxation process. The moving ion leaves a dense cloud behind it. The nonequilibrium density takes a finite time to relax to an equilibrium bulk density through transitional diffusion. This process gives rise extra drag on the motion of the ion.[32,64−67] Stiles and Hubbard[32] have extended the Hubbard−Onsager model to include a first-order correction for electrostriction around an ion in a compressible solvent. They derived a quantity, $(e^2/16\pi\epsilon_0\epsilon_r)(\partial \ln \epsilon_r/\partial p)_T[3\rho_0(\partial \ln \eta_0/\partial\rho_0)_T - 1]$, where p is pressure, that can be used to measure the electrostrictive component of the viscous friction. The Stiles and Hubbard model predicts significant augmentation of the drag coefficient of ions in a compressible solvent which usually has positive values of $(\partial \ln \epsilon_r/\partial p)_T$ and $3\rho_0(\partial \ln \eta_0/\partial\rho_0)_T > 1$. We found that this model significantly overestimated the friction coefficients at conditions where the compressibility of the solvent is large and fails to provide a quantitative representation of the experimental limiting conductance data. We note that the expression given by Stiles and Hubbard is only valid for large ions for which both dielectric friction and electrostriction are not too large, so it is not directly applicable to the present calculation.

4. Conclusion

Despite the many approximations in the present model, it predicts all the qualitative features of the temperature and density variation of the limiting conductance of aqueous NaCl solution with $\rho_0 > 0.4$−0.5 g cm^{-3}. These features include weak isochoric temperature dependence at $T > 656$ K, the decrease of the Walden product with the decrease of the density, and the similarity of Λ_0 for all alkali halides (small ions). With only one adjustable parameter, this model can reproduce all the experimental limiting conductance data for NaCl for $\rho_0 > 0.5$ g cm^{-3} and from 413 K $< T <$ 1073 K within about the experimental uncertainty. The success of this model is attributed to the consideration of both electrostriction and the electroviscous effect which are very large under these conditions. In the absence of a more rigorous model the present model seems to account approximately for the major effects in aqueous solutions at high temperature. Similar success might be expected in any solvent near and above its critical point.

Acknowledgment. The authors thank J. B. Hubbard for his suggestions for improving the manuscript and J. M. H. Levelt Sengers and D. G. Friend for the helpful discussions about the viscosity of water at high densities. C.X. thanks Eric M. Yezdimer and Shinichi Sakane for their help with Mathematica This work was supported by the National Science Foundation under Grant CHE 9725163.

References and Notes

(1) Noyes, A. A. *The Electrical Conductivity of Aqueous Solutions*; Carnegie Institution of Washington: Washington, DC, 1907; Publication No. 63.
(2) Franck, E. U. *Z. Phys. Chem. (Munich)* **1956**, *8*, 92.
(3) Franck, E. U. *Z. Phys. Chem. (Munich)* **1956**, *8*, 107.
(4) Franck, E. U. *Z. Phys. Chem. (Munich)* **1956**, *8*, 192.
(5) Hartmann, D.; Franck, E. U. *Ber. Bunsen-Ges. Phys. Chem.* **1969**, *73*, 514.
(6) Mangold, K.; Franck, E. U. *Ber. Bunsen-Ges. Phys. Chem.* **1969**, *73*, 21.
(7) Renkert, H.; Franck, E. U. *Ber. Bunsen-Ges. Phys. Chem.* **1970**, *74*, 40.
(8) Dunn, L. A.; Marshall, W. L. *J. Phys. Chem.* **1969**, *73*, 723.
(9) Frantz, J. D.; Marshall, W. L. *Am. J. Sci.* **1984**, *284*, 651.
(10) Quist, A. S.; Franck, E. U.; Jolly, H. R.; Marshall, W. L. *J. Phys. Chem.* **1963**, *67*, 2453.
(11) Quist, A. S.; Marshall, W. L. *J. Phys. Chem.* **1966**, *70*, 3714.
(12) Quist, A. S.; Marshall, W. L. *J. Phys. Chem.* **1968**, *72*, 684.
(13) Quist, A. S.; Marshall, W. L. *J. Phys. Chem.* **1968**, *72*, 2100.
(14) Quist, A. S.; Marshall, W. L. *J. Phys. Chem.* **1969**, *73*, 978.
(15) Fogo, J. K.; Benson, S. W.; Copland, C. S. *Rev. Sci. Instrum.* **1951**, *22*, 276.
(16) Fogo, J. K.; Benson, S. W.; Copland, C. S. *J. Phys. Chem*. **1954**, *22*, 212.
(17) Pearson, D.; Copland, C. S.; Benson, S. W. *J. Am. Chem. Soc.* **1963**, *85*, 1044.
(18) Ho, P. C.; Palmer, D. A.; Mesmer, R. E. *J. Solution Chem.* **1994**, *23*, 997.
(19) Zimmerman, G, H.; Gruszkiewicz, M. S.; Wood, R. H. *J. Phys. Chem.* **1995**, *99*, 11612.
(20) Gruszkiewicz, M. S.; Wood, R. H. *J. Phys. Chem.* **1997**, *101*, 6549.
(21) Bockris, J. O'M.; Reddy, A. K. N. *Modern Electrochemistry*; Plenum: New York, 1970; Vol. 1.
(22) Kay, R. L. In *Water—A Comprehensive Treatise*; Franks, F., Ed.; Plenum: New York, 1973; Vol. 3.
(23) Chong, C.; Hirata, F. *J. Chem. Phys*. **1998**, *108*, 7339.
(24) Korneshan, S.; Lynden-Bell, R. M.; Rasaiah, J. C. *J. Am. Chem. Soc*. **1998**, *120*, 12041.
(25) Oelkers, E. H.; Helgeson, H. C. *Geochim. Cosmochim. Acta* **1988**, *52*, 63.
(26) Born, M. *Z. Phys.* **1920**, *1*, 221.
(27) Boyd, R. H. *J. Phys. Phys.* **1961**, *35*, 1603; **1970**, *39*, 2376.
(28) Zwanzig, R. *J. Chem. Phys.* **1963**, *38*, 1603.
(29) Zwanzig, R. *J. Chem. Phys.* **1970**, *67*, 4850.
(30) Hubbard, J. B.; Onsager, L. *J. Chem. Phys.* **1977**, *67*, 4850.
(31) Hubbard, J. B. *J. Chem. Phys*. **1978**, *68*, 1649.
(32) Stiles, P. J.; Hubbard, J. B. *Chem. Phys. Lett*. **1984**, *105*, 655.
(33) Wood, R. H.; Carter, R. W.; Quint, J. R.; Majer, V.; Thompson, P. T.; Boccio, J. R. *J. Chem. Thermodyn.* **1994**, *26*, 225.
(34) Quint, J. R.; Wood, R. H. *J. Phys. Chem*. **1985**, *89*, 380.
(35) Frank, H. S. *J. Chem. Phys.* **1955**, *23*, 2023.
(36) Booth, F. J. *J. Chem. Phys*. **1951**, *19*, 391.
(37) Luo, H.; Tucker, S. C. *J. Phys. Chem.* **1996**, *100*, 11165.
(38) Luo, H.; Tucker, S. C. *J. Phys. Chem. B* **1997**, *101*, 1063.
(39) Wolynes, P. G. *Annu. Rev. Phys. Chem*. **1980**, *31*, 345.
(40) Brillianto, N. V.; Krapivsky, P. L. *J. Phys. Chem.* **1991**, *95*, 6055.
(41) Kestin, J.; Sengers, J. V.; Kamgar-Parsi, B.; Sengers, J. M. L. *J. Phys. Chem. Ref. Data* **1984**, *13*, 175.
(42) Rønne, C.; Thrane, L.; Åstrand, P.; Wallqvist, A.; Mikkelsen, K. V.; Keiding, S. R. *J. Chem. Phys.* **1997**, *107*, 5319.
(43) Loef, J. J. *Physica* **1981**, *103B*, 133.
(44) Quist, A. S.; Marshall, W. L. *J. Phys. Chem*. **1965**, *69*, 2984.
(45) Okada, K.; Imashuku, Y.; Yao, M. *J. Chem. Phys.* **1997**, *107*, 9302.
(46) Okada, K.; Yao, M.; Hiejima, Y.; Kohno, H.; Kajihara, Y. *J. Chem. Phys*. **1999**, *110*, 3026.
(47) Lee, S. H.; Cummings, P. T.; Simonson, J. M.; Mesmer, R. E. *Chem. Phys. Lett.* **1998**, *293*, 289.
(48) Hirschfelder, J. O.; Curtiss, C. F. *Molecular Theory of Gases and Liquids*; John Wiley & Sons: New York, 1954.
(49) Balbuena, P.; Johnston, K. P.; Rossky, P. J.; Hyun, J. *J. Phys. Chem. B* 1997.
(50) Ibuki, K.; Nakahara, M. *J. Chem. Phys.* **1986**, *84*, 2776.
(51) Ho, P. C.; Palmer, D. A. *Geochim. Cosmochim. Acta* **1997**, *61*, 3027.
(52) Ho, P. C.; Palmer, D. A. *J. Solution Chem.* **1995**, *24*, 753.
(53) Shock, H. L.; Helgeson, H. C. *Geochim. Cosmochim. Acta* **1988**, *52*, 2009.
(54) Xiao, C.; Tremaine, P. R. *J. Solution Chem*. **1997**, *26*, 277.
(55) Wolynes, P. G. *J. Chem. Phys.* **1978**, *68*, 473.
(56) Bagchi, B. *J. Chem. Phys*. **1991**, *95*, 467.
(57) Biswas, R.; Bagchi, B. *J. Chem. Phys*. **1997**, *106*, 5597.
(58) Impey, R. W.; Madden, P. A.; McDonld, S. A. *J. Phys. Chem.* **1983**, *87*, 7, 5071.
(59) Nguyen, H. L.; Adelman, S. A. *J. Chem. Phys*. **1984**, *81*, 4564.
(60) Wilson, M. A.; Pohorille, A.; Pratt, L. R. *J. Chem. Phys.* **1985**, *83*, 5382.
(61) Lee, S. H.; Rasaiah, J. C. *J. Chem. Phys*. **1994**, *101*, 6964.
(62) Lee, S. H.; Rasaiah, J. C. *J. Phys. Chem*. **1996**, *100*, 1420.
(63) Koneshan, S.; Rasaiah, J. C.; Lynden-Bell, R. M.; Lee, S. H. *J. Phys. Chem. B* **1998**, *102*, 4193.
(64) Hubbard, J. B.; Wolynes, P. G. In *The Chemical Physics of Solvation, Part C: Solvation Phenomena in Specific Chemical, Physical and Biological Systems*; Dogonadze, R. R., Kalman, E., Kornyshev, A. A., Ulstrup, J., Eds.; Elsevier: New York, 1988; pp 3—112.
(65) Van der Zwan, G.; Hynes, J. T. *Physica A* **1983**, *121*, 227.
(66) Chen, J.-H.; Adelman, S. A. *J. Chem. Phys.* **1980**, *72*, 2819.
(67) Colonomos, P.; Wolynes, P. G. *J. Chem. Phys*. **1978**, *71*, 2644.